

# Quantum circuits for floating-point arithmetic

Thomas Haener<sup>1,3</sup>, Mathias Soeken<sup>2</sup>, Martin Roetteler<sup>3</sup>, and Krysta M. Svore<sup>3</sup>

<sup>1</sup>ETH Zürich, Zürich, Switzerland

<sup>2</sup>EPFL, Lausanne, Switzerland

<sup>3</sup>Microsoft, Redmond, WA, USA

**Abstract.** Quantum algorithms to solve practical problems in quantum chemistry, materials science, and matrix inversion often involve a significant amount of arithmetic operations which act on a superposition of inputs. These have to be compiled to a set of fault-tolerant low-level operations and throughout this translation process, the compiler aims to come close to the Pareto-optimal front between the number of required qubits and the depth of the resulting circuit. In this paper, we provide quantum circuits for floating-point addition and multiplication which we find using two vastly different approaches. The first approach is to automatically generate circuits from classical Verilog implementations using synthesis tools and the second is to generate and optimize these circuits by hand. We compare our two approaches and provide evidence that floating-point arithmetic is a viable candidate for use in quantum computing, at least for typical scientific applications, where addition operations usually do not dominate the computation. All our circuits were constructed and tested using the software tools LIQUi| and RevKit.

## 1 Introduction

Quantum computing shows great promise for solving classically intractable computational problems. The wide range of potential applications includes factoring [1], quantum chemistry [2, 3], and linear systems of equations [4]. Most of these quantum algorithms invoke subroutines which carry out a classical computation on a superposition of exponentially many input states. Examples include modular exponentiation for factoring [1], evaluating orbital functions for quantum chemistry (e.g., linear combinations of Gaussians) [2], and reciprocals for solving systems of linear equations [4]. While large-scale quantum computers able to run such algorithms are not yet available, it is nevertheless crucial to analyze the resulting circuits in order to acquire resource estimates. These can then guide further development of both quantum algorithms and hardware, allowing for efficient hardware-software co-design.

For instance, recent quantum algorithms to simulate quantum chemistry models implement time evolution under the electronic structure Hamiltonian of electrons interacting with nuclei and with each other. Mathematically, this is described by the Hamiltonian

$$H = - \sum_i \nabla_i^2 / 2 - \sum_{i,j} \frac{Z_i}{|R_i - r_j|} + \sum_{j>i} \frac{1}{|r_i - r_j|},$$

where  $\nabla_i^2$  is the Laplace operator of electron  $i$ , the vectors  $R_i$  denote the locations of the nuclei, the scalars  $Z_i$  denote the charges of the nuclei, and the  $r_i$  are vectors describing the locations of the electrons. When calculating the two-electron integrals of the Hamiltonian  $H$  in order to compute the representation of  $H$  in second quantization on-the-fly, expressions such as  $1/|r_i - r_j|$  must be evaluated. In recent approaches such as [2] these expressions would have to be evaluated in superposition, i.e., a quantum circuit is required that computes for instance  $x \mapsto 1/x$ , where  $x$  is a representation of the underlying distances. Also the inverse square root operator  $x \mapsto 1/\sqrt{x}$  naturally appears in these computations as typically a computation of Euclidean distances is involved. Several choices seem possible to represent inputs and outputs to these operations, including fixed-point and floating-point representations. Here, we focus on studying the impact of different choices of floating-point representations on the number of quantum bits (qubits) and number of  $T$ -gates that are required for basic arithmetic operations such as addition and multiplication, from which then more involved operations such as  $1/x$  and  $1/\sqrt{x}$  can be built, e.g., via Newton's method.

Compared to a fixed-point representation, floating-point arithmetic offers great savings in number of qubits when the required range of values and/or relative precision is large. Thus, finding good circuits for floating-point arithmetic could be of tremendous use in many applications of quantum computing.

This paper is organized as follows: After a short introduction to floating-point arithmetic and quantum circuits in Sect. 2 and Sect. 3, we employ state-of-the-art synthesis tools to transform classical, non IEEE-compliant Verilog implementations to optimized reversible circuits and present the results in Sect. 4. We then introduce our hand-optimized circuits in Sect. 5 and mention advantages and disadvantages of using an automatic synthesis approach as opposed to optimizing by hand in Sect. 6. Finally, in Sect. 7, we provide evidence for the viability of using floating-point arithmetic in quantum computing and give a summary and outlook in Sect. 8.

## 2 Floating-point addition and multiplication

In a floating-point representation, every number  $x$  is approximated using three registers: 1 sign bit  $x_S$ ,  $M$  bits for the (non-negative) mantissa  $x_M$  (a number in  $[1, 2)$ ), and  $E$  bits for the exponent  $x_E$ . Then,

$$x \approx (-1)^{x_S} x_M \cdot 2^{x_E}$$

and because  $x_M \in [1, 2)$ , its highest bit is always 1 and therefore it need not be stored explicitly. This format allows to represent a much larger range of values with a given number of bits than a fixed-point representation. Yet, basic arithmetic operations require more gates due to the extra steps involved to align and re-normalize intermediate results. In particular, adding two floating-point numbers  $x = (x_S, x_M, x_E)$  and  $y = (y_S, y_M, y_E)$  involves the following steps:

1. If  $x_E < y_E$ , swap the two floating-point numbers.
2. Compute two's complement from sign bits and mantissas (including the implicit leading 1).
3. Align the two results according to the difference in exponents  $\Delta_E = x_E - y_E$  (only if  $|\Delta_E| < M$ , else the addition will have no effect).
4. Add mantissas in two's complement.
5. Translate from two's complement to sign bit and mantissa.
6. If adding the two mantissas caused an overflow, right-shift the result by 1 and increment the exponent.
7. Determine the position of the first 1. Left-shift the mantissa by that amount and then update the exponent accordingly.
8. When copying out the result, check if there was over/underflow in the exponent and output infinity or 0, respectively.

Multiplying two floating-point numbers  $x$  and  $y$ , on the other hand, is much simpler because there is only one renormalization step involved. In summary, it requires the following steps:

1. Determine result exponent  $r_E = x_E + y_E$ .
2. Multiply mantissas (including the implicit leading 1) into a  $2M$ -bit register.
3. If there was overflow, right-shift by 1 and increment the result exponent.
4. If  $x_E < 0$  and  $y_E < 0$  but  $r_E > 0$ , output 0.
5. If  $x_E \geq 0$  and  $y_E \geq 0$  but  $r_E < 0$ , output infinity.
6. Determine the sign bit of the result.

While both floating-point operations are more expensive than their fixed-point analog, the overhead is much more prominent for addition. This fact will have important consequences for our discussion about the practicality of floating-point representations in quantum computing, which we will present in Sect. 7.

### 3 Quantum circuits

Programs which run on a quantum computer can be described using quantum circuit diagrams, similar to the one depicted in Fig. 1b. Each line represents a qubit and the program is executed from left to right. Because the time evolution of a closed quantum system is described by a unitary operator, every quantum instruction must be reversible (note that this does not include measurement). In particular, executing classical functions on a quantum computer requires mapping all classical non-reversible gates to Toffoli gates (doubly-controlled NOTs) acting on quantum bits. Furthermore, intermediate results need to be stored in temporary work qubits (ancilla qubits) in order to render the computation reversible.

Once the program has been compiled for a certain hardware architecture, the resulting instructions can be executed on the target device. However, physical implementations of qubits are far from perfect and the resulting noise would corrupt the output of any quantum program of nontrivial size. This problem

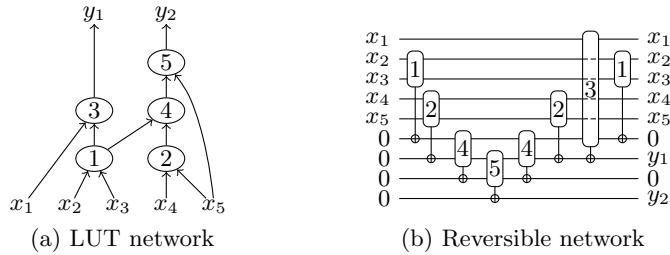


**Fig. 1.** Translation of LUT networks into reversible networks with single-target gates

can be remedied by employing quantum error correction which encodes a single logical qubit using many physical ones and thereby reduces the effects of noise on the computation. In order to use quantum error correction, however, all quantum operations need to be mapped to a discrete gate set. One such set of operations is called Clifford+ $T$ , where the  $T$ -gate is usually the most expensive quantum operation. There are several proposals to implement a  $T$ -gate, and all of them feature a large overhead in terms of physical qubits. By, e.g., having many  $T$ -gate factories available, the runtime of a quantum program can be estimated from the  $T$ -depth. To estimate the overhead in  $T$ -gate factories, also the number of  $T$ -gates which must be executed in parallel is an important measure. In combination with the number of logical qubits, these measures typically allow for a good estimate of the overall cost. We therefore provide these measures for all our circuits. In addition, we provide the circuit size [5]

$$KQ = T\text{-depth} \cdot \#\text{Qubits} ,$$

which can be used to compare different implementations.

## 4 Automatic circuit synthesis

In this section, we present cost estimates for both floating-point addition and multiplication based on reversible networks that are obtained from the LUT-based hierarchical synthesis approach (LHRS, [6]). LHRS reads as input a classical gate-level logic network, e.g., provided as Verilog file. It then uses LUT mapping techniques (e.g., [7–9]) from conventional logic synthesis algorithms to map the gate-level netlist into a LUT network composed of  $k$ -input LUT gates, which can realize any  $k$ -input Boolean function. An example for a LUT network where  $k = 2$  is illustrated in Fig. 1a. Such a network is translated into a reversible network composed of single-target gates. Single-target gates are generalized reversible gates in which the value of a target line is inverted if a given Boolean control function evaluates to true on the control line values of the gate. Fig. 1b depicts one possible result of such a translation. Intermediate values are stored on ancillae, which are initialized 0 and need to be restored to their initial value after computation. The order in which the LUTs are traversed in this translation affects the number of required ancillae, because an early uncomputation of

**Table 1.** Resource counts for the automatically generated circuits.

Design	Width	Qubits	$T$ -count	Runtime
Adder	16	76	112,059,924	143.49
Adder	16	100	40,915	2.28
Adder	32	239	79,415	24.22
Adder	64	538	165,509	2.05
Mult	16	81	3,195,745	3276.00
Mult	32	351	1,110,133	238.82
Mult	64	1675	7,709,931	3318.67

ancilla allows to reuse them for other intermediate values. The aim is to find a reversible network with as few ancillae as possible. In the reversible network each single-target gates is mapped to a Clifford+ $T$  network. For this purpose, different algorithms have been proposed [10, 6].

To obtain circuits using LHRS we first optimized existing IP blocks for floating-point addition and multiplication for gate count and mapped them into AND-inverter graphs (AIGs), which are logic networks that are composed of AND gates and inverters. We configured the IP blocks in a way that their functionality is as close to the functionality of the hand-optimized circuits. That is, the IP blocks are not IEEE compliant and rounding is always closest to zero. The obtained AIG representation is used as starting point for the initial  $k$ -LUT mapping. As value for  $k$ , we used the smallest value such that the number of required qubits does not exceed the number of qubits obtained from the hand-optimized circuits. To find that value, one can run LHRS without mapping the single-target gates into Clifford+ $T$  networks. This step is typically quite fast, and the runtime required for it can be neglected.

For each single-target gate, we used all available mappers and compared the quality of the resulting Clifford+ $T$  networks, then taking the best one. A plot of the parameters of several solutions for the case of 16-bit floating-point adders is shown in Fig. 2. These circuits, as well as the circuits in Table 1 which improve over some of the results obtained in [6] were generated using RevKit, which has implementations of direct XMG-based synthesis (DXS, [11]), circuit-based synthesis (CBS, [12]), and LHRS.

## 5 Hand-optimized circuits

In this section, we present hand-optimized circuits for both floating-point addition and multiplication. We detail the individual circuit components and provide resource estimates in order to compare to the synthesis approach discussed in Sect. 4.

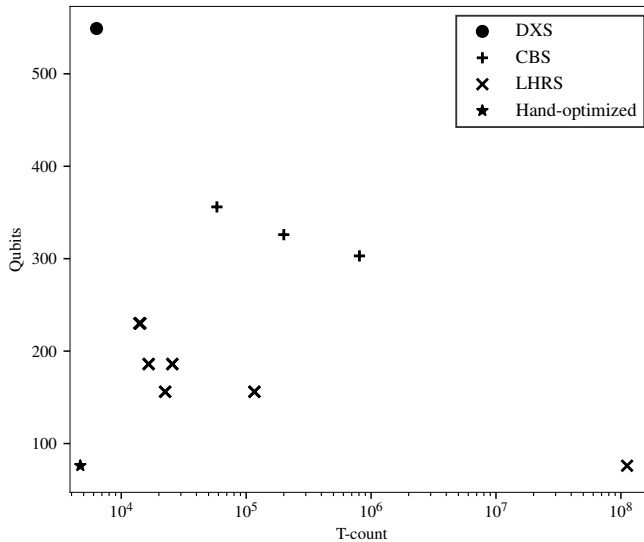


**Fig. 2.** Plot of characteristics of different implementations of 16-bit floating-point implementations, based on resource counts provided in [6]. Each point corresponds to the number of qubits and number of  $T$ -gates for a particular circuit generated via different circuit synthesis methods, including LHRS. The data point for the hand-crafted circuit is located in the bottom left corner.

### 5.1 Basic building blocks

Our hand-generated floating-point circuits consist of a series of basic building blocks. We use the integer adder from Ref. [13] and construct an integer multiplier from it using the standard shift-and-add approach. To compare two  $n$ -bit numbers, we perform a subtraction using one extra qubit (i.e., on  $n + 1$  bits), followed by an addition without this extra qubit, which holds the result of the comparison. If the comparison involves a classically-known constant, we use the CARRY circuit from Ref. [14].

The only floating-point-specific blocks are the ones used to determine the location of the first one in a bit-string, and to shift the mantissa by an amount  $s$  (specified in an input register). More specifically, the first circuit achieves the mapping

$$|x\rangle |0\rangle \xrightarrow{F} |x\rangle | \lfloor \log_2(x) \rfloor \rangle ,$$

where  $x$  is interpreted as a positive integer. The shift circuits  $S^\pm$  perform the mapping

$$|s\rangle |x\rangle \xrightarrow{S^\pm} |s\rangle |2^{\pm s}x\rangle .$$

In this case,  $x$  is a  $2M$ -bit register, where the first/last  $M$  bits are guaranteed to be zero, and  $s$  is a  $\log_2 M$ -bit register representing the shift.

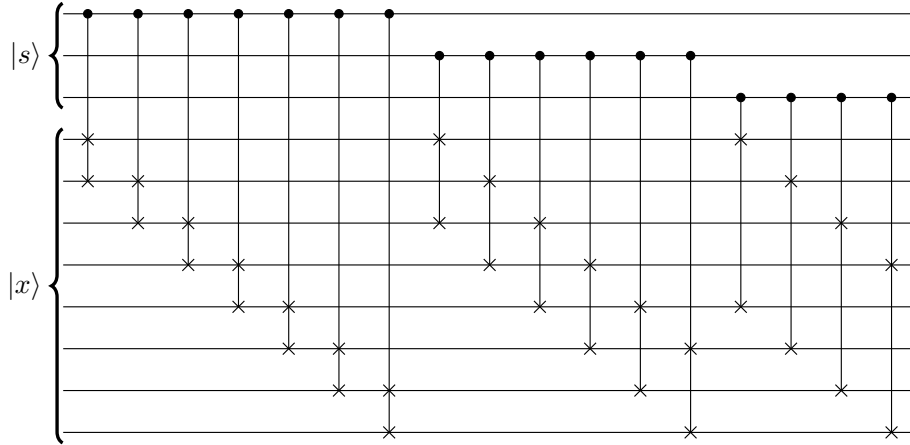


**Fig. 3.** Implementation of a shift circuit for an 8-bit number  $x$ . The shift  $s$  must be such that the top, i.e., least-significant  $s$  bits of  $x$  are 0. Variations of this circuit are required to enable shifts in both directions and to ensure that the sign bit is copied when right-shifting a negative number in two's complement.

## 5.2 Implementation

A straight-forward implementation of these shift circuits  $S^\pm$  would, for every  $m \in \{0, \dots, M - 1\}$ , copy out the  $M$ -bit value  $x$  shifted by  $m$  bits into a new  $2M$ -bit register, conditional on  $s$  being equal to  $m$ .

To save  $M$  qubits,  $x$  can first be padded with  $M$  bits to the left/right. This allows exchanging the copy-operations above with swaps: For each  $m \in \{1, \dots, M - 1\}$ , the bits of  $x$  can be swapped  $m$  bits to the left/right, starting at the left-/right-most bit. Yet, this approach requires  $M(M - 1)$  Fredkin gates.

A more efficient implementation can be obtained by swapping the bits of  $x$  to the left/right by  $2^k$ , conditional on the  $k$ -th bit of the shift-register  $|s\rangle$  and repeating this for every  $k \in \{0, \dots, \log_2 M - 1\}$ . An example circuit for a 3-bit shift register and an 8-bit  $x$ -register is depicted in Fig. 3. In general, this circuit requires  $\mathcal{O}(M \log_2 M)$  Fredkin gates for a  $\log_2 M$ -sized shift-register.

Finding the first one, i.e., implementing the  $F$  operation mentioned above, can be achieved using a circuit similar to the one in Fig. 4, which depicts an example for 8 bits. The flag  $f$  being 1 indicates that the first 1 in the bit-representation of  $x$  has not yet been found. For every bit  $x_i$  of  $x$  (starting with bit-index  $i = 0$ ), the position register is initialized to  $i$  if the flag is 1 and  $x_i = 1$  (i.e., it is the first 1). Then, the flag-bit is flipped conditional on the position register being equal to the current  $i$  (note that only positive controls need to be placed on the position register).

All of the required components were implemented and thoroughly tested using a reversible simulator extension to LIQUi| [15]. The high-level overview circuits for both floating-point addition and multiplication are depicted in Fig. 5

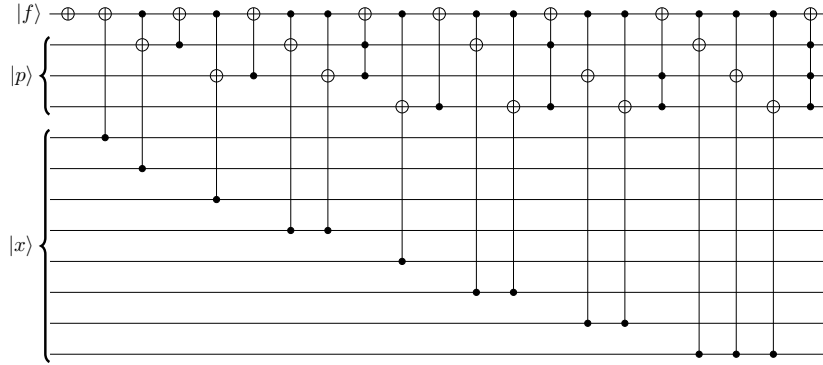


**Fig. 4.** Circuit for finding the first one in the bit-representation of  $x$ . The flag  $f$  (which is initially set to 1 using the first NOT gate) is toggled to 0 as soon as the first 1 has been found. The position of the first one is stored in the  $p$ -register, consisting of 3 bits in this example.

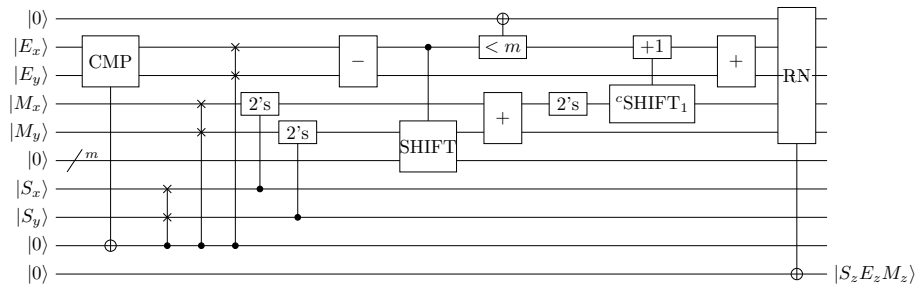


**Fig. 5.** High-level overview of the floating-point addition circuit. First, the inputs are sorted by the exponent (comparison followed by controlled swaps). Then, the second mantissa is shifted by the difference of the exponents before it is added to the first mantissa and converted back from two's complement (taking the pseudo-sign bit as the new sign bit). If there was a final carry in the addition, the result is shifted by 1 bit and the exponent is incremented by 1. The final RN gate renormalizes the intermediate result using the first-ones circuit (see Fig. 4) followed by shifting the mantissa (see Fig. 3) by the output of the first-ones circuit and copies out the resulting floating-point representation, taking care of zero and infinity outcomes.



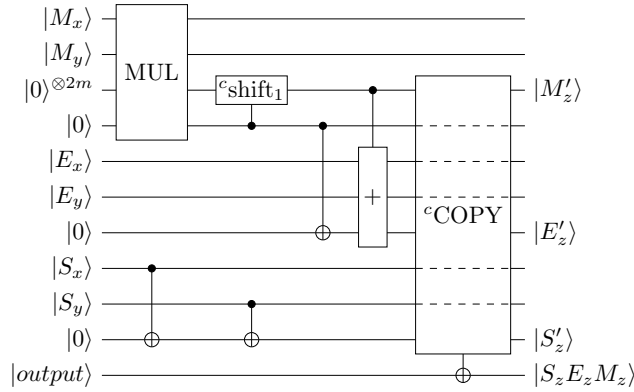


**Fig. 6.** High-level overview of the floating-point multiplication circuit. After multiplying the input mantissas  $M_x$  and  $M_y$  into a new register of  $2m$  qubits ( $m$  denotes the number of mantissa bits), it is right-shifted by one if the resulting mantissa  $M_x \cdot M_y \geq 2$ . The exponent is updated accordingly (using a CNOT), followed by an addition of both input exponents  $E_x$  and  $E_y$  into  $E'_z$  (if  $M_x \cdot M_y \neq 0$ ). The final step denoted by  ${}^c\text{COPY}$  consists of conditionally copying out of the resulting exponent, mantissa and sign bit to take care of special cases such as over- and underflows in computing the resulting exponent which turn to infinity and zero outcomes, respectively.

and Fig. 6 and the resource counts which resulted from the implementation in  $\text{LIQUi}| \rangle$  can be found in Table 2.

## 6 Advantages and disadvantages of automatic circuit synthesis

The results in the previous sections showed that the cost resulting from the hand-crafted floating-point addition and multiplication circuits are clearly much lower than the cost resulting from the automatic synthesis tool. The main reason for this discrepancy is that the synthesis algorithm is agnostic to the type of design. The synthesis approach does not use the fact that a floating-point operation contains a characteristic structure, as it is exploited in finding the hand-crafted designs. It also highly depends on the logic network that is input to the synthesis algorithm. In our case, this has been optimized in order to reduce the area (in terms of number of gates) in conventional circuits. The relation of this objective to the number of qubits and  $T$ -count is not fully understood—finding a correlation and deriving a corresponding cost function from it will significantly boost the effectiveness of the automatic synthesis approach.

Nevertheless, automatic synthesis has clear advantages already in its current implementation:

Design	Width	Qubits	$T$ -count	$T$ -depth
Adder	16	76	4,704	1,386
Adder	32	140	11,144	3,138
Adder	64	268	26,348	7,224
Mult	16	81	6,328	2,580
Mult	32	158	26,642	11,154
Mult	64	315	122,752	52,116

**Table 2.** Resource counts for the hand-optimized circuits. Each Toffoli gate was decomposed using 7 T-gates [16] in  $T$ -depth 3, providing an upper-bound on the actual T-count [17].

1. One can apply automatic synthesis to various designs and get immediate results. In contrast, to derive a high-quality hand-crafted design can require several months.
2. Automatic synthesis can find various different implementations of the same design by adjusting the synthesis parameters. This allows for design space exploration. Depending on the targeted quantum platform or the context of the design inside a quantum algorithm, one can address different objectives.
3. One may be able to find a design that requires fewer qubits. Reducing the number of quantum operations, e.g.,  $T$  gates, in post-synthesis optimization algorithms is much easier than reducing the number of qubits. Automatic synthesis techniques can in principle find quantum circuits without any ancilla qubits (except to store the result of the outputs). For example, the 16-bit variants of the floating-point adder and multiplier would require only 48 qubits. Although such a circuit is likely to have a very large number of quantum operations, the circuit provides a good starting point for post-synthesis optimization.

## 7 Practicality of floating-point arithmetic for quantum computing

While the automatic synthesis approach in its current implementation produces very large circuits, floating-point arithmetic for quantum computing is still a viable option, at least when using hand-optimized circuits. Most likely, there are still further improvements possible also in our hand-optimized design: While it features a much lower circuit width than previous adders such as the 32-bit floating-point adder presented in Ref. [18], the  $T$ -depth of our design is larger. Specifically, our design requires 1/6 of the number of qubits of the adder in Ref. [18] and features a size of

$$\begin{aligned}
 KQ &= T\text{-depth} \cdot \#\text{Qubits} \\
 &\leq 439,320 ,
 \end{aligned}$$

which is still a 39.3% improvement over the  $KQ = 723,301$  reported in Ref. [18], despite the much larger  $T$ -depth.

Furthermore, we argue that exchanging fixed-point arithmetic in a given computation by floating-point arithmetic will result in a circuit of similar cost: While the resource requirements of floating-point addition are much larger than for fixed-point numbers, it is important to note that the cost of floating-point multiplication is very similar to performing it in a fixed-point representation, and given that multiplication in both representations is more expensive than addition, the measure of choice should actually be the cost of multiplication. Furthermore, most applications feature similar numbers of additions and multiplications and often, they can even be combined into a single fused multiply-add instruction which is true, e.g., when evaluating polynomials using the Horner scheme [19]. This means that the overhead of using floating-point arithmetic for applications where multiplications and additions are balanced or where multiplication even dominate is actually much less than what is generally expected. The KQ ratio between a 32-bit floating-point multiplier and a 24-bit fixed-point multiplier (where we require intermediate results to be computed for the full  $2M$  bits) is

$$\frac{KQ_{\text{float}}^{\text{mul}}}{KQ_{\text{fixed}}^{\text{mul}}} = \frac{11,154 \cdot 158}{10,656 \cdot 5 \cdot 24} \approx 1.38 ,$$

which clearly shows that the circuit sizes are similar, even for such an unfair comparison: While the chosen bit-sizes guarantee the same absolute precision if no exponent is used, the floating-point multiplier can deal with a much wider range of values at constant relative error. Considering a scientific application with roughly equal numbers of additions and multiplications will cause a deviation from the calculated overhead above by at most another factor of two, since additions require less resources regardless of the chosen representation.

Therefore, we conclude that the cost of using floating-point arithmetic is not only manageable, but that it actually incurs almost no overhead for typical scientific applications. For many quantum algorithms, the extra range and constant relative error offered by a floating-point representation are well worth an increase in circuit size of 2-3 $\times$ .

## 8 Summary and outlook

Given the strict requirements of the IEEE standard, it is expected that IEEE-compliant floating-point arithmetic features large overheads compared to fixed-point arithmetic. Furthermore, even when considering non IEEE-compliant blocks, the number of gates obtained from circuit synthesis is much larger than what would be expected from a fixed-point implementation. Yet, in combination with manual circuit optimization, relaxing the requirements allows for significant savings in both width and size of the circuit, rendering the use of floating-point arithmetic for future quantum devices much more practical. Furthermore, since

the cost of multiplying fixed-point numbers is very similar to floating-point multiplication, using floating-point arithmetic in typical scientific applications will incur an overhead in the circuit size  $KQ$  of only  $2\text{-}3\times$ .

One reason for the large discrepancy between our two approaches—manual optimization and automatic circuit synthesis—is that the objective function used in the optimization process for classical computing is very different from the one used in quantum computing: In classical computing, the most costly resource is time, while bits are essentially free. Circuits resulting from an optimization procedure aiming to minimize the cost function for classical computing are thus highly parallel, but they also require more bits. In quantum computing, on the other hand, both circuit depth and width (i.e., number of bits) are precious resources [5]. This makes introducing parallelism harder and an optimization procedure would generate vastly different circuits featuring less parallelism and fewer bits.

While the hand-optimized circuits require fewer qubits and  $T$ -gates, it is very likely that some of the subroutines may still be further optimized using methods from the automatic synthesis approach. Furthermore, the interplay among different components in the hand-written circuit may benefit from such a procedure. We aim to investigate this combination of approaches in future work.

## References

1. Peter W. Shor. Algorithms for quantum computation: Discrete logarithms and factoring. In *Foundations of Computer Science, 1994 Proceedings., 35th Annual Symposium on*, pages 124–134. IEEE, 1994.
2. Ryan Babbush, Dominic W. Berry, Ian D. Kivlichan, Annie Y. Wei, Peter J. Love, and Alán Aspuru-Guzik. Exponentially more precise quantum simulation of fermions in second quantization. *New Journal of Physics*, 18(3):033032, 2016.
3. Markus Reiher, Nathan Wiebe, Krysta M. Svore, Dave Wecker, and Matthias Troyer. Elucidating reaction mechanisms on quantum computers. *arXiv:1605.03590*, 2016.
4. Aram W. Harrow, Avinatan Hassidim, and Seth Lloyd. Quantum algorithm for linear systems of equations. *Physical review letters*, 103(15):150502, 2009.
5. Andrew M. Steane. Overhead and noise threshold of fault-tolerant quantum error correction. *Physical Review A*, 68(4):042322, 2003.
6. Mathias Soeken, Martin Roetteler, Nathan Wiebe, and Giovanni De Micheli. Hierarchical reversible logic synthesis using LUTs. In *Design Automation Conference*, pages 78:1–78:6. ACM, 2017.
7. Jason Cong and Yuzheng Ding. FlowMap: an optimal technology mapping algorithm for delay optimization in lookup-table based FPGA designs. *IEEE Trans. on CAD of Integrated Circuits and Systems*, 13(1):1–12, 1994.
8. Deming Chen and Jason Cong. DAomap: a depth-optimal area optimization mapping algorithm for FPGA designs. In *Int'l Conf. on Computer-Aided Design*, pages 752–759, 2004.
9. Sayak Ray, Alan Mishchenko, Niklas Eén, Robert K. Brayton, Stephen Jang, and Chao Chen. Mapping into LUT structures. In *Design, Automation and Test in Europe*, pages 1579–1584, 2012.

10. Nabila Abdessaied, Mathias Soeken, and Rolf Drechsler. Technology mapping for single target gate based circuits using Boolean functional decomposition. In *Int'l Conf. on Reversible Computation*, pages 219–232, 2015.
11. Mathias Soeken, Martin Roetteler, Nathan Wiebe, and Giovanni De Micheli. Design automation and design space exploration for quantum computers. In *Design, Automation and Test in Europe*, pages 470–475. IEEE, 2017.
12. Mathias Soeken and Anupam Chattopadhyay. Unlocking efficiency and scalability of reversible logic synthesis using conventional logic synthesis. In *Design Automation Conference*, pages 149:1–149:6, 2016.
13. Yasuhiro Takahashi, Seiichiro Tani, and Noboru Kunihiro. Quantum addition circuits and unbounded fan-out. *arXiv preprint arXiv:0910.2530*, 2009.
14. Thomas Häner, Martin Roetteler, and Krysta M. Svore. Factoring using  $2n+2$  qubits with Toffoli based modular multiplication. *Quantum Information and Computation*, 17(7 & 8), 2017.
15. Dave Wecker and Krysta M. Svore. LIQ*U*i|>: A software design architecture and domain-specific language for quantum computing. *arXiv*, 1402.4467, 2014.
16. Michael A. Nielsen and Isaac L. Chuang. *Quantum Computation and Quantum Information*. Cambridge University Press, 2000.
17. Cody Jones. Low-overhead constructions for the fault-tolerant Toffoli gate. *Physical Review A*, 87(2):022328, 2013.
18. Trung Duc Nguyen and Rodney Van Meter. A resource-efficient design for a reversible floating point adder in quantum computing. *ACM Journal on Emerging Technologies in Computing Systems*, 11(2):13:1–13:18, 2014.
19. Donald E Knuth. Evaluation of polynomials by computer. *Communications of the ACM*, 5(12):595–599, 1962.